




Article

Profiled Horn Antenna with Wideband Capability Targeting Sub-THz Applications

Jay Gupta ¹, Dhaval Pujara ^{1,*} and Jorge Teniente ²

¹ Department of Electronics and Communication Engineering, Institute of Technology, Nirma University, Ahmedabad 382481, India; 16ftvphde14@nirmauni.ac.in

² Antenna Group & Institute of Smart Cities (ISC), Electric, Electronic and Communication Engineering Department, Public University of Navarra, Campus de Arrosadia, E-31006 Pamplona, Spain; jorge.teniente@unavarra.es

* Correspondence: dhaval.pujara@nirmauni.ac.in

Abstract: This paper proposes a wideband profiled horn antenna designed using the piecewise biarc Hermite polynomial interpolation and validated experimentally at 55 GHz. The proposed design proves S_{11} and directivity better than -22 dB and 25.5 dB across the entire band and only needs 3 node points if compared with the well-known spline profiled horn antenna. Our design makes use of an increasing radius and hence does not present non-accessible regions from the aperture, allowing its fabrication with electro erosion techniques especially suitable for millimeter and submillimeter wavelengths.

Keywords: electro erosion; Hermite polynomial interpolation; profiled smooth circular waveguide horn; plasma diagnostics; spline profile



check for updates

Citation: Gupta, J.; Pujara, D.; Teniente, J. Profiled Horn Antenna with Wideband Capability Targeting Sub-THz Applications. *Electronics* **2021**, *10*, 412. <https://doi.org/10.3390/electronics10040412>

Academic Editors: Rashid Mirzavand, Mohammad Saeid Ghaffarian and Mohammad Mahdi Honari
Received: 16 December 2020
Accepted: 5 February 2021
Published: 8 February 2021

Publisher's Note: MDPI stays neutral with regard to jurisdictional claims in published maps and institutional affiliations.



Copyright: © 2021 by the authors. Licensee MDPI, Basel, Switzerland. This article is an open access article distributed under the terms and conditions of the Creative Commons Attribution (CC BY) license (<https://creativecommons.org/licenses/by/4.0/>).

1. Introduction

Horn antennas are widely used for applications such as radio astronomy, satellite, and terrestrial communication, plasma diagnostics, etc. A detailed description of different horn antenna configurations was provided by Olver and Clarricoats [1]. Many researchers have proposed novel horn designs, including Potter horns [2], corrugated horns [3], matched-feed horns [4], dielectric horns [5–7], metamaterial horns [8], etc., with an aim to improve the radiation performance of horn antennas, reducing their size, manufacturing complexity, optimization time, etc. Among various horn antenna options, the corrugated horn antenna is widely used due to several advantages. However, due to a complex mode-converter structure, the radial corrugated horn design becomes challenging especially at millimeter and submillimeter waves [9] and terahertz frequencies [10]. Some of the alternative solutions are axial corrugated horn [11,12], hybrid corrugated horn [13,14], spline profiled horn [9,15], and horn antennas designed using interpolation [16]. All such configurations have their merits and drawbacks in terms of performance, fabrication complexity, cost, computational effort, etc.

This paper describes the design, fabrication, and measurement of a profiled smooth circular waveguide horn antenna. This horn antenna has been designed using biarc Hermite polynomial interpolation with only 3 node points. The simulated results for this horn are compared with a spline profiled horn [9] to achieve the same performance. The horn has been designed for D-band with potential application in the reflectometry system for plasma diagnostics. The reflectometry system has stringent antenna specifications in terms of high directivity, suppressed sidelobes, and Gaussian-like radiation characteristics. More details on antennas for the plasma diagnostics system can be found in [17]. Based on the performance comparison of various D-band profiles, two of the horn profiles are scaled-down to the V-band frequencies for testing reasons. Then, the V-band horns are fabricated, and the radiation performance has been verified and compared with simulations.

This paper is divided into six sections. Section 2 discusses the design and geometry of the horn antenna design using biarc Hermite polynomial interpolation method. Moreover, the importance of the proposed profile compared to the spline profile is included. Section 3 includes the comparative study of the performance of various biarc Hermite polynomial interpolation profile options. Section 4 describes the scaled-down model of the D-band horn antenna and the fabrication of the V-band horn antenna. The comparison of measured results with that of the simulated ones is covered in Section 5. In Section 6, conclusions are derived.

2. Profiled Smooth Circular Waveguide Horn Design Using Biarc Hermite Polynomial Interpolation

Polynomial interpolation is a method of estimating mid-points between the known data points with successive tangents [18]. As a part of curve fitting, many interpolation methods [19], such as spline, trigonometric, Birkhoff, multivariate, Hermite interpolation, etc., can be chosen to connect the selected node points. These techniques may help in smoothening the curvature of a profiled horn antenna design.

As compared to the spline profile [9,15], the profile using polynomial interpolation has more degrees of freedom with less intermediate node points and this aspect is very important to reduce computation time. To develop a similar kind of curved/wavy profile as the one we are presenting in the following paragraphs, having a comparable performance with spline interpolation, at least 9 node points (7 intermediate and 2 end node points) are required, which increases the optimization time and resources if spline profile design method is to be used.

It is important to remark that, a spline profiled horn antenna optimized using a large number of node points can obtain a very good radiation performance with the cost of optimization time. However, it is very challenging to fabricate it or even impossible using electro erosion techniques, since it may have flare angle changes with non-accessible zones from the aperture, and it usually presents a wavy internal profile. There are other manufacturing techniques as the ones that make use of a lathe which can solve this problem, but as frequency increases and approximates the end of the millimeter-wave frequency band, they are not accurate enough except expensive electroforming fabrication techniques; but we want to avoid these techniques due to cost restrictions. The profile results with non-accessible regions in case of spline interpolation since the radius of the successive node points may have a smaller value than that of the preceding ones. Due to this, it is very difficult and time-consuming optimization for a spline profiled horn antenna, to maintain the radius of the successive node points in increasing order since the curve between nodes is somewhat wavy due to the nature of spline interpolation technique. To overcome these limitations, we propose a new profile formulation in this paper which also presents a lower number of node points, i.e., 3, and then reduces computation time.

It is important to remark that for millimeter and submillimeter waves, manufacturing by electro erosion techniques is very suitable for a tiny smooth-walled horn antenna. This is because the roughness of electro erosion surface finish that can be limiting in terms of losses for other feed components; it does not impact too much in horn antenna losses since a proper design in terms of length and slopes maintains the electric fields far from metallic walls except in the throat region with a small reduction in aperture efficiency that usually is not very important for these tiny horns. Only mechanical post-processing in the manufacturing of these tiny horns is usually needed for the input waveguide part, where the strength of the fields in the metallic walls is higher, but this can be solved usually by finishing the horn with a smaller circular waveguide and ream post-processing to the final input circular waveguide size. This manufacturing method is not expensive, and the result can be very nice compared to split-block manufacturing techniques where the alignment between both parts can be critical at upper frequencies of the millimeter wavelengths and submillimeter wavelengths. If we compare electro erosion manufacture with electroforming manufacturing techniques which are very suitable for these frequencies, the cost reduction is high. This is probably one of the main advantages of the profile optimization technique

indicated in this paper as it has been explained in the previous paragraph. The proposed profile allows direct manufacturing by electro-erosion and a reduction in the optimization complexity. It is to be noted that to employ the electrical discharge machining (EDM) technique, the horn antenna profile must present a decreasing profile from the aperture. Hence, spline profile having non-accessible parts cannot be manufactured using this technology.

In Reference [16], the authors of this paper have presented the preliminary design of the profiled horn antenna using Hermite polynomial interpolation approach. The geometry for the same is shown in Figure 1. It has two node points P_1 and P_2 , one at the throat section and the other at the aperture section of the horn, respectively. Both node points are taken as origin, i.e., $(0, 0)$ for the individual sections of the horn. Here, \vec{n}_1 is the principal unit normal vector point made by connecting points P_1 and (x_1, y_1) . Similarly, \vec{n}_2 is made by connecting the points P_2 and (x_2, y_2) . \vec{t}_1 is the tangent vector to \vec{n}_1 and \vec{t}_2 is for \vec{n}_2 . In Hermite polynomial interpolation, successive tangents ($\vec{t}_{s1}, \vec{t}_{s2}, \dots, \vec{t}_{sn}$) are generated in order to connect \vec{t}_1 with \vec{t}_2 as shown in Figure 1.

As may be seen in Figure 1, the input radius is " r_{in} ", the aperture radius is " r_{ap} ", and " L " is the length of the horn. The region between the vectors \vec{n}_1 and \vec{t}_1 at throat section is indicated by " Δ ", and the region between \vec{n}_2 and \vec{t}_2 at aperture section is indicated by " \blacktriangle ". The mathematical formulation explained above is important to reconstruct/optimize/improve the profile. This profile can be designed with the Curve Fitting Toolbox that uses MATLAB function "`rscvn`", making a planar piecewise biarc Hermite interpolation curve.

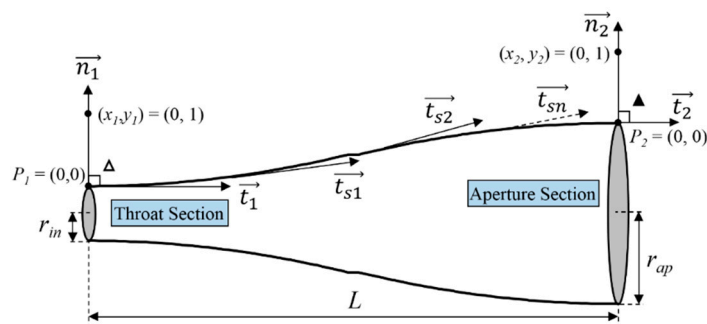


Figure 1. Geometry of the proposed profile smooth circular waveguide horn (with 2 node points) designed using biarc Hermite polynomial interpolation with principal unit normal vector points as $(x_1, y_1) = (x_2, y_2) = (0, 1)$; $r_{in} = 0.8$ mm; $r_{ap} = 8.50$ mm; $L = 50$ mm for a center frequency of 140 GHz [16].

The profile of the horn antenna discussed in Figure 1 is used to make a mirror image profile as shown in Figure 2. The complete profile is developed in two equal parts of length $L/2$ each. The necessary steps to form the geometry are listed below:

Step 1: The first half of the profile indicated as "I" is the replica of the profile shown in Figure 1. It should be clear that the profiling is exactly the same; however, the length and radius are different as indicated in Figure 2.

Step 2: "I" is mirror-imaged to form "II".

Step 3: "II" is horizontally flipped to form "III", i.e., the second half of the mirror image profile.

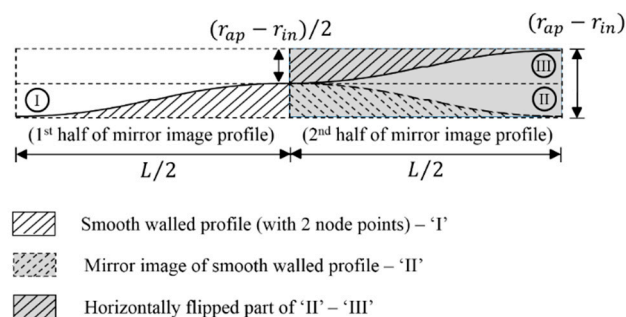


Figure 2. Steps to design a mirror image profile.

Using the mirror-imaged profile shown in Figure 2, the proposed horn antenna (having 3 node points) is designed as shown in Figure 3. To formulate the profile having 3 node points, one can use the flip array functions (in MATLAB) on the 2 nodes profile. Once it is done, the second part (flipped one) is to be clubbed with the first one as demonstrated in Figure 2.

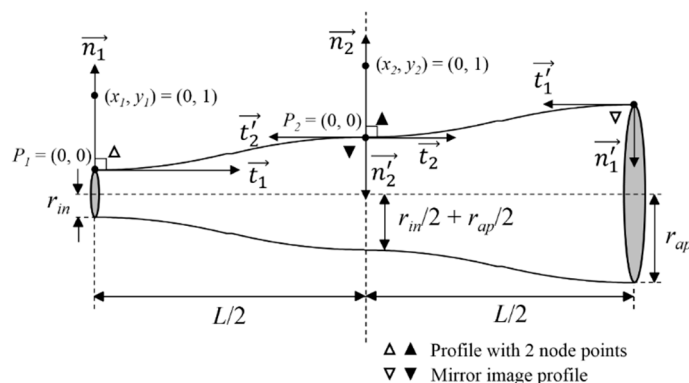


Figure 3. Geometry of mirror image profile horn antenna (having 3 node points) using biarc Hermite polynomial interpolation with principal unit normal vector points as $(x_1, y_1) = (x_2, y_2) = (0, 1)$; $r_{in} = 0.8$ mm; $r_{ap} = 8.50$ mm; $L = 50$ mm for center frequency of 140 GHz.

Here, \vec{n}'_1 and \vec{n}'_2 are the principal unit normal vector points for the second half of the geometry and are inverted vectors of \vec{n}_1 and \vec{n}_2 , respectively. Similarly, \vec{t}'_1 and \vec{t}'_2 are the inverted tangent vectors of \vec{t}_1 and \vec{t}_2 , respectively. The symbols “▼” and “▽” indicate the regions for the second half of the geometries. The radius at the center of the profile is $r_{in}/2 + r_{ap}/2$.

3. Comparative Study of the Performance of Various Profile Options

In the case of spline horn [9] with 9 node points, the number of optimization variables, i.e., the radii of the intermediate node points are 7; this value turned out to be the minimum number of node points to achieve similar performance. The proposed profile has 3 node points and can be optimized using only two variables, i.e., (x_1, y_1) and (x_2, y_2) , the principal unit normal vector points. By changing the location of these vectors, their corresponding vectors \vec{n}'_1 and \vec{n}'_2 vary; this in turn results in a change of their tangent vectors accordingly. Since this profile is controlled by the vectors (not by the radius of the intermediate node points), its successive node points will not have a smaller radius than the preceding one, as in the case of spline optimization and this is very important at least for electro erosion manufacture techniques. To clarify, the main difference of this technique is that really the profile is not made over multiple radii but over the inclination of the profile sections which has several advantages for manufacturing techniques drawn before.

Different locations of the principal unit normal vector points under consideration are shown in Table 1. The different profiles with 2 node points are shown in Figure 4a where x_1 and x_2 are varied from -0.4 to 0 with a step of 0.1 while y_1 and y_2 are kept constant as 1 . The same concept is applied for the mirror image profiled horn antenna in order to carry out the comparative study. Different profiles for the same are shown in Figure 4b.

Table 1. Values of unit normal vector points for various profiling options.

Principal Unit Normal Vector Points	
(x_1, y_1)	(x_2, y_2)
$(0, 1)$	
$(-0.1, 1)$	
$(-0.2, 1)$	$(0, 1); (-0.1, 1); (-0.2, 1); (-0.3, 1); (-0.4, 1)$
$(-0.3, 1)$	
$(-0.4, 1)$	

Accordingly, using this interpolation technique, all the possible geometries of the horn antenna are designed and simulated using the commercially available antenna design software—Ansys HFSS and CHAMP by TICRA. Figure 5 shows the influence on the directivity of the profiled horn antenna (having 3 node points) due to variation in the values of x_1 and x_2 .

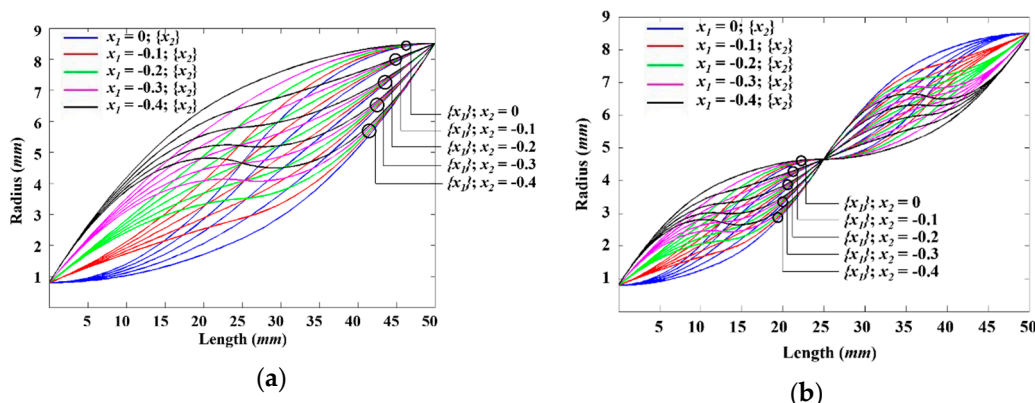


Figure 4. Different profiling options for (x_1, y_1) and (x_2, y_2) as $(\{x_1\}, 1)$ and $(\{x_2\}, 1)$. (a) Profile possibilities with 2 node points; (b) mirror image profile possibilities with 3 node points.

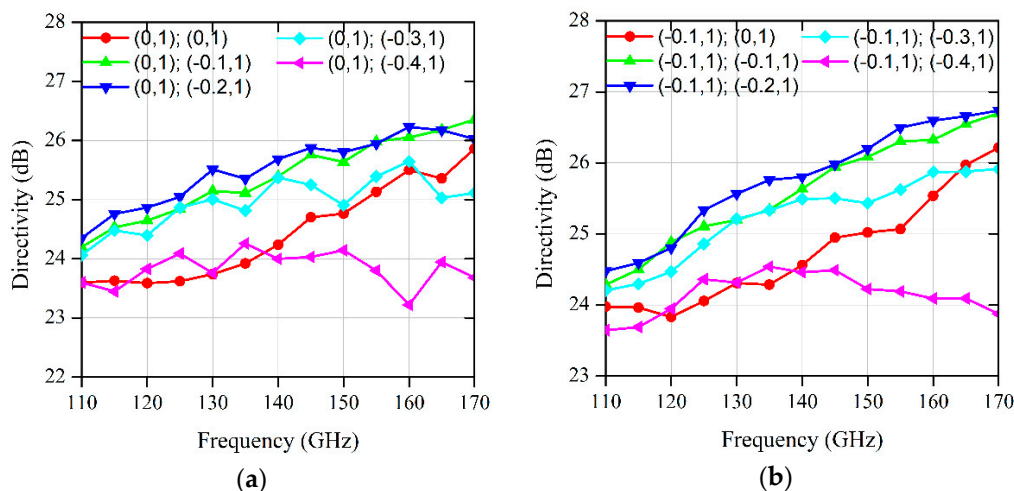


Figure 5. Cont.

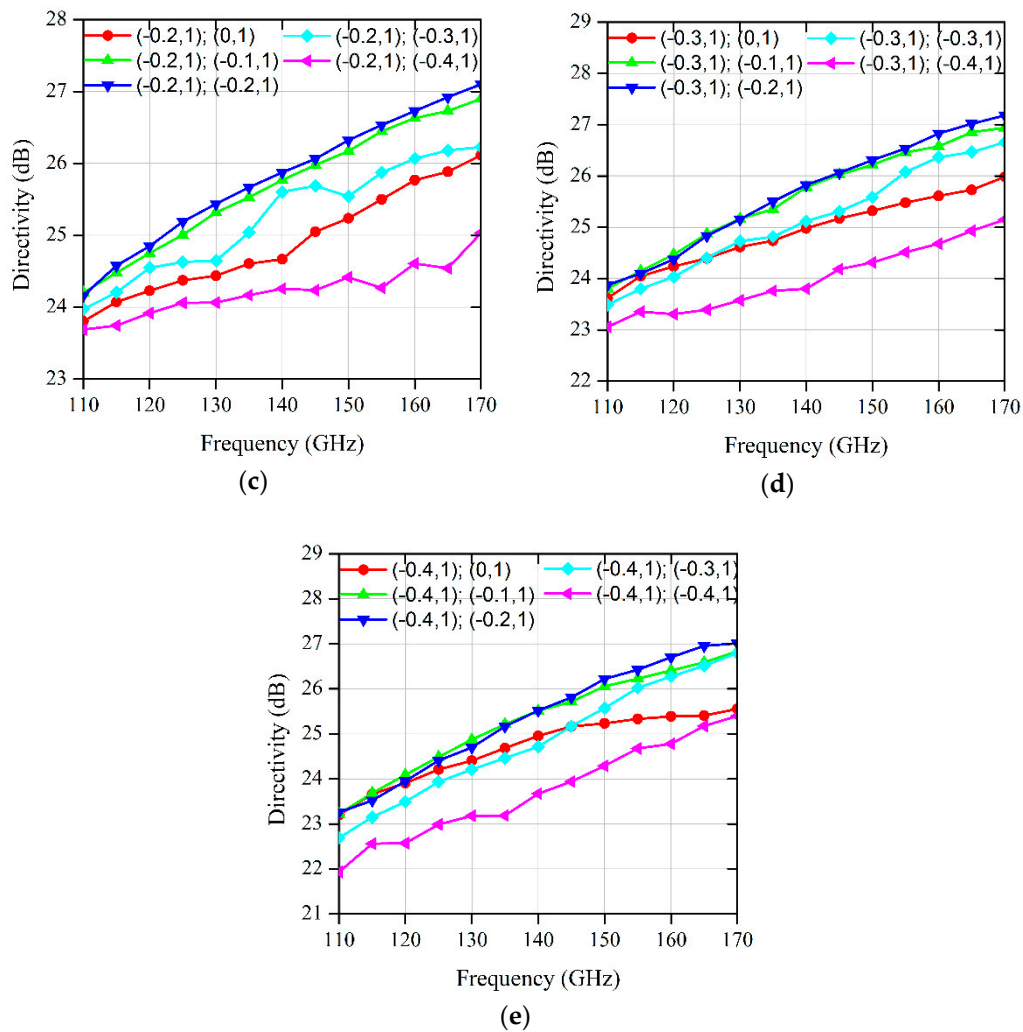


Figure 5. Directivity index (dB) by varying the position of principal unit normal vector points (x_1, y_1) and (x_2, y_2) as (a) $(0, 1)$ and $(\{x_2\}, 1)$; (b) $(-0.1, 1)$ and $(\{x_2\}, 1)$; (c) $(-0.2, 1)$ and $(\{x_2\}, 1)$; (d) $(-0.3, 1)$ and $(\{x_2\}, 1)$; (e) $(-0.4, 1)$ and $(\{x_2\}, 1)$.

By observing the obtained results, it can be seen that the directivity is improved for the middle values of x_2 and has the best performance when x_2 is around -0.2 and -0.1 . It is also important to remark that the variation along the band can be modulated with x_1 and the variation is less when x_1 equal to -0.1 . As this value is reduced, the directivity is reduced for lower frequencies of the band and increased for higher frequencies of the band. The comparative results in terms of directivity at 140 GHz for horn antennas with 2 and 3 node points are shown in Figure 6. Similarly, the performance of the profiles having 2 and 3 node points in terms of the spillover efficiency for different taper levels is shown in Figures 7 and 8, respectively. It can be seen from the results that the spillover performance is more dependent on the variation of the vectors at the aperture side. It can be improved when the vectors at the aperture end create more opening, and it is reduced while the profiles are wavier in nature.

In the case of profiles having 2 node points, there is a trade-off between directivity and spillover performance. However, in the case of profiles having 3 node points, both the performance characteristics can be improved when the values of x_2 is around -0.2 ; this means that this value of x_2 is quite interesting, to begin with. Moreover, the modal analysis of different profiles has been carried out. The normalized power in TE and TM modes at the aperture of these horn antennas is as shown in Figure 9. Here, only power distribution in TE_{11} , TE_{12} , and TM_{11} are shown, as they are having almost 99% of the total input power. From the simulated modal distribution, it can be seen that the hybrid mode

(HE₁₁) is propagating through a horn antenna for a particular design region (when x_2 is around -0.2 and -0.1) which results in better performance. Moreover, it can be observed how the variation in profiling is affecting the modal distribution in repetitive nature. In other words, the modal distribution for any particular value of x_1 with variation in x_2 has a repetitive nature for different values of x_1 . Based on the result analysis, Figure 10 includes the Region of Interest (RoI) proposed for designing the mirror image profile horn antenna. It is defined only for the middle of the profile, as the performance is less influenced by variation in the values of x_1 .

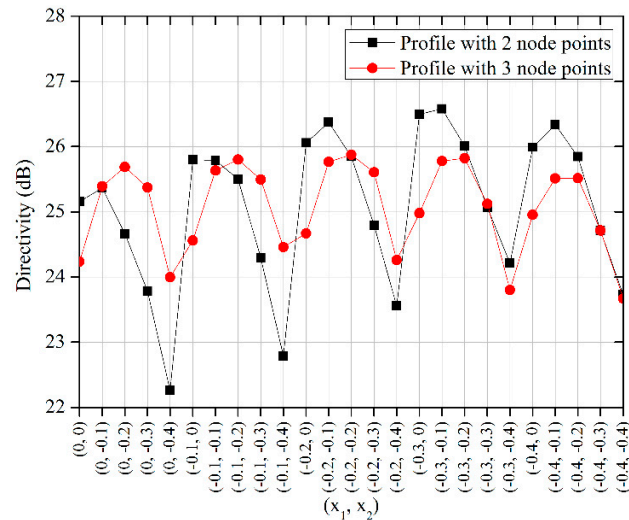


Figure 6. Comparison of directivity (at 140 GHz) for horn antennas with 2 and 3 node points.

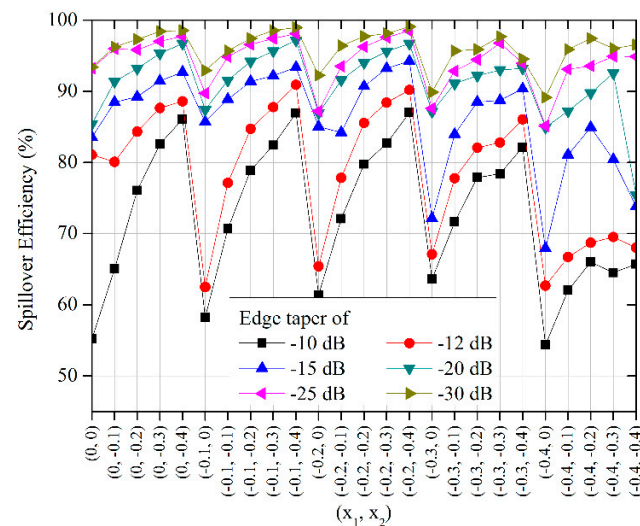


Figure 7. Comparison of directivity (at 140 GHz) for horn antennas with 2 and 3 node points.

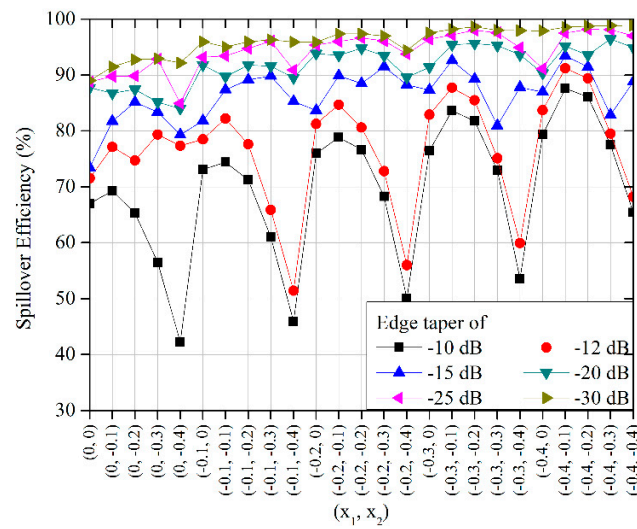


Figure 8. Comparison of spillover efficiency for several edge tapers (at 140 GHz) for horn antennas with 3 node points.

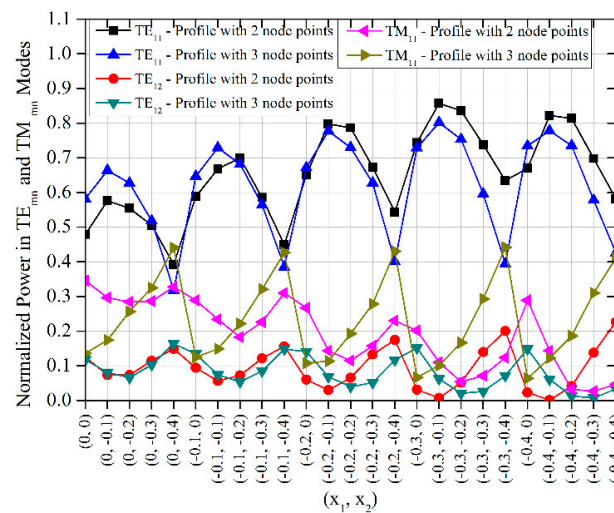


Figure 9. Normalized power in TE_{mn} and TM_{mn} modes for different values of x_1 and x_2 .

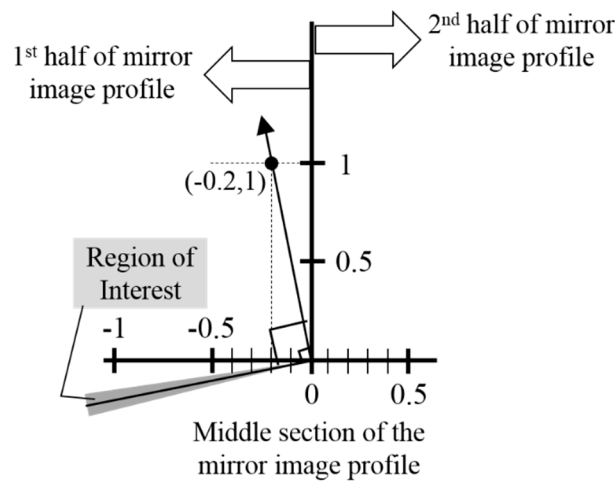


Figure 10. RoI at the middle section of the profile for designing the mirror image profile horn antenna.

Further, to obtain the cutoff frequency for TE and TM modes for the circular waveguide, Equations (1) and (2) can be used, respectively.

$$f_{c, mn} = \frac{1}{2\pi\sqrt{\epsilon\mu}} \frac{p'_{mn}}{a}, \tag{1}$$

$$f_{c, mn} = \frac{1}{2\pi\sqrt{\epsilon\mu}} \frac{p_{mn}}{a}, \tag{2}$$

where, $f_{c, mn}$ is the cut off frequency; m is the number of full wave patterns along the circumference; n is the number of half wave patterns along the diameter; ϵ is the permittivity of the medium; μ is the permeability of the medium; a is the radius of the circular waveguide; p_{mn} is the n th zero of Bessel function $J_m(k_c a)$; p'_{mn} is the n th zero of $J'_m(k_c a)$, i.e., the first derivative of the Bessel function; k_c is the cut off wave number.

The values of zeros of $J'_m(k_c a)$ and $J_m(k_c a)$ for TE and TM modes are given in Tables 2 and 3, respectively.

Table 2. Values of p'_{mn} for TE modes of circular waveguide.

$J'_m(k_c a)=0$	$n = 1$	$n = 2$	$n = 3$
$m = 0$	0	3.8317	7.0156
$m = 1$	1.8412	5.3314	8.5363
$m = 2$	3.0542	6.7061	9.9695

Table 3. Values of p_{mn} for TM modes of circular waveguide.

$J_m(k_c a)=0$	$n = 1$	$n = 2$	$n = 3$
$m = 0$	2.4048	5.5201	8.6537
$m = 1$	3.8317	7.0156	10.1735
$m = 2$	5.1356	8.4172	11.6198

Putting different values of the zeros of the Bessel function to the equations, one can find the lowest cutoff frequency. Hence, it becomes clear that the TE₁₁ mode is the dominant mode in case of the circular waveguide. Other higher order modes can be calculated using Equations (1) and (2). The series of the circular waveguide modes can be seen in Figure 11.

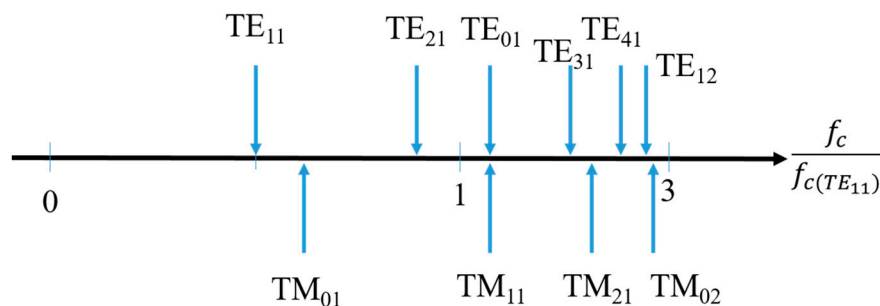


Figure 11. Mode series for the circular waveguide.

It should be clear that the RoI shown in Figure 10 is for the first half of the total profile; the second half will automatically be formed with the mirror image concept, as explained in Section 2. In this paper, the profiles are optimized for the directivity and spillover efficiency in case of the profiles having 2 and 3 node points. Further, it can be optimized for the various radiation characteristics such as cross-polarization. Moreover, new profiles can be designed by increasing the node points or by introducing some other techniques like multiple mirrored geometry.

4. Scaled-Down Models of D-Band Horn Antennas

In the above section, the simulated results for various profiles of the D-band (110–170 GHz) horn antennas are discussed. To verify the simulated performance with the measurement results, two scaled-down horns at V-band (one having 2 and another with 3 nodes) have been manufactured. Figure 12 shows the simulation design as well as the manufactured horn antennas. Scaling has been done to reduce the fabrication complexity and cost of D-band antennas and allow measurement with our available facilities. It should be noted that the scaling does not change any radiation characteristics or modal content, and the performance of V-band horns would be identical to the D-band horns. The high-frequency horn is simply converted to the lower band by using a multiplication factor. Accordingly, the geometrical parameters of the scaled-down model (V-band) are calculated and shown in Table 4. The values for the principal unit normal vector points (x_1, y_1) ; (x_2, y_2) are $(-0.2, 1)$; $(-0.1, 1)$ and $(-0.3, 1)$; $(-0.2, 1)$ for the profiles having 2 and 3 node points, respectively.

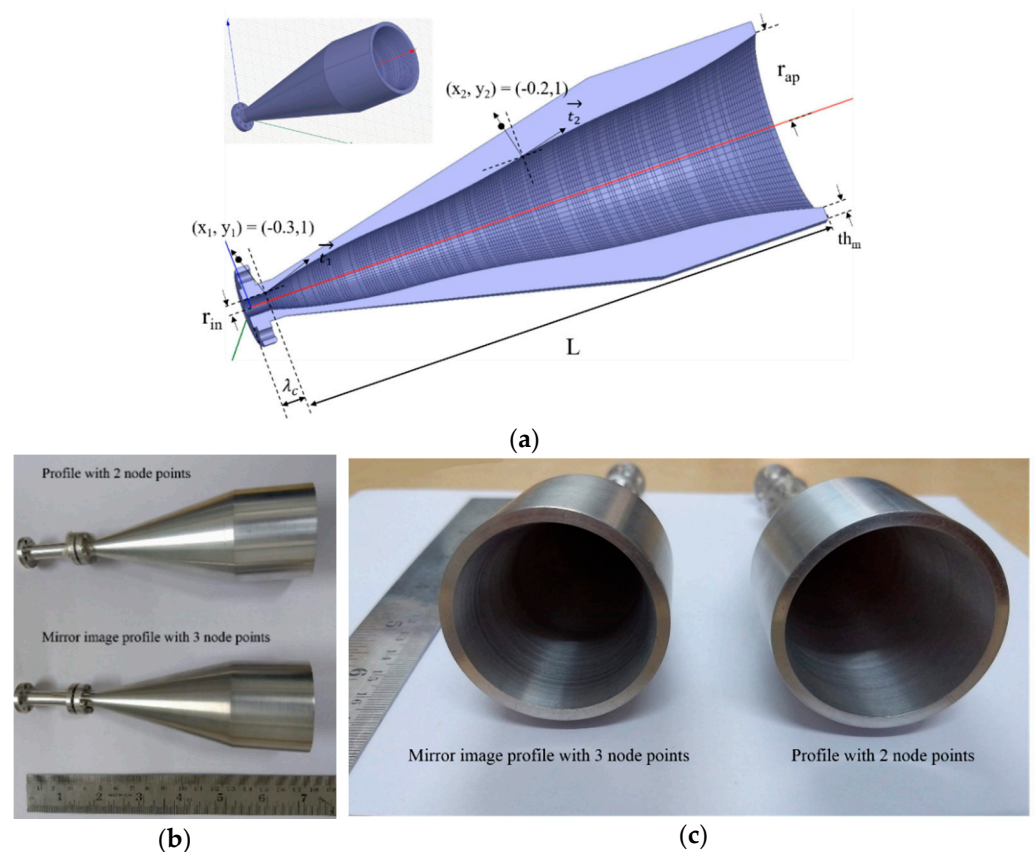


Figure 12. Photographs of the (a) simulated design of V-band horn having 3 node points ($th_m = 3$ mm, $\lambda_c = 5.45$ mm); fabricated V-band horn antennas with 2 and 3 node points (b) lateral view (c) front view.

Table 4. Geometrical parameters of the scaled-down model (scaling factor = 2.545).

Geometrical Parameter	Values in mm
r_{in}	2.09
r_{ap}	21.67
L	127.26

The performance of the fabricated horn antennas has been measured at the Space Applications Centre, Indian Space Research Organisation (SAC-ISRO), Ahmedabad.

5. Results and Discussion

In this section, simulated and measured performance for the proposed smooth circular waveguide horn designed using the piecewise biarc Hermite polynomial interpolation (having 2 and 3 node points) are compared with that of a spline horn. The spline profile is designed using spline curve fitting formulae such that it follows the curvature of the proposed profile. As discussed in the previous section, the spline profile requires 9 nodes to follow the curvature like the one proposed. All the profiles (with 2 and 3 node points and spline profile with 9 node points) designed at V-band are shown in Figure 13. The comparative results in terms of S_{11} (dB) are as shown in Figure 14.

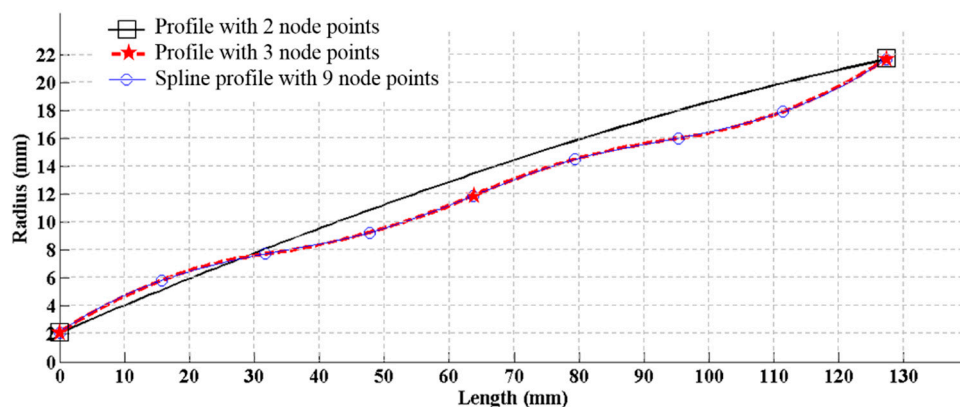


Figure 13. Comparison of profiles with 2 and 3 node points and 9 nodes spline profile horn.

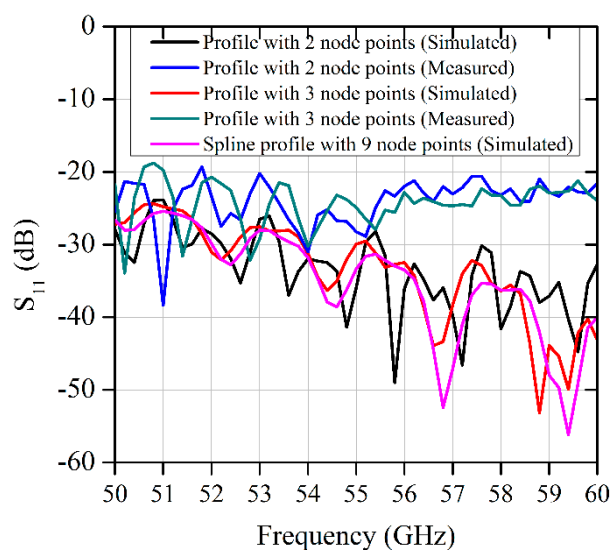


Figure 14. Comparison of simulated (Ansys HFSS) and measured S_{11} (dB) for profiled horn antenna with 2 and 3 node points and 9 nodes spline profile horn.

From Figure 14, it is evident that simulated results are in close agreement and measured results present a worse performance at higher frequencies but still acceptable. This difference may be due to fabrication and/or calibration measurement error uncertainties.

Similarly, the radiation patterns were measured for the fabricated horn antennas. The photograph of the radiation pattern measurement setup is shown in Figure 15. The antennas were measured in a rollover azimuth far-field range. The measured radiation patterns and directivity of both the antennas (profiles having 2 and 3 node points) are compared with the simulated spline profile horn as shown in Figures 16 and 17, respectively. As discussed, the profile is optimized only for the directivity and spillover performances. Hence, the other radiation characteristics like cross-polarization are not covered in the

results. However, the worst cross-polarization isolation for $\varphi = 45^\circ$ plane is better than -20 dB.

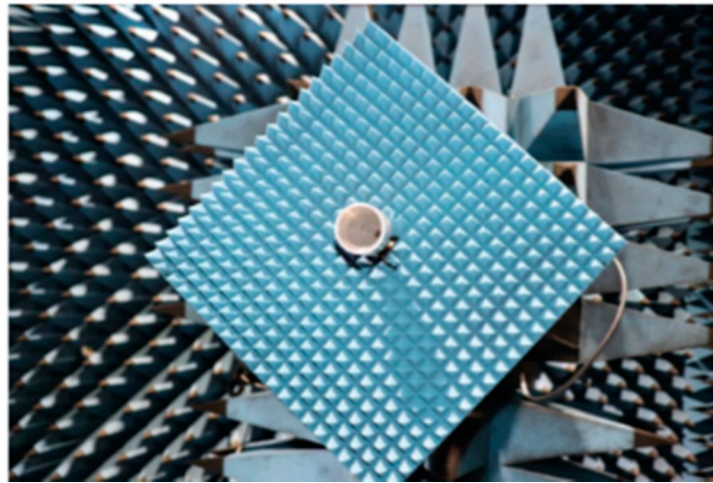


Figure 15. Photograph of the radiation pattern measurement setup of horn antennas at SAC-ISRO facility.

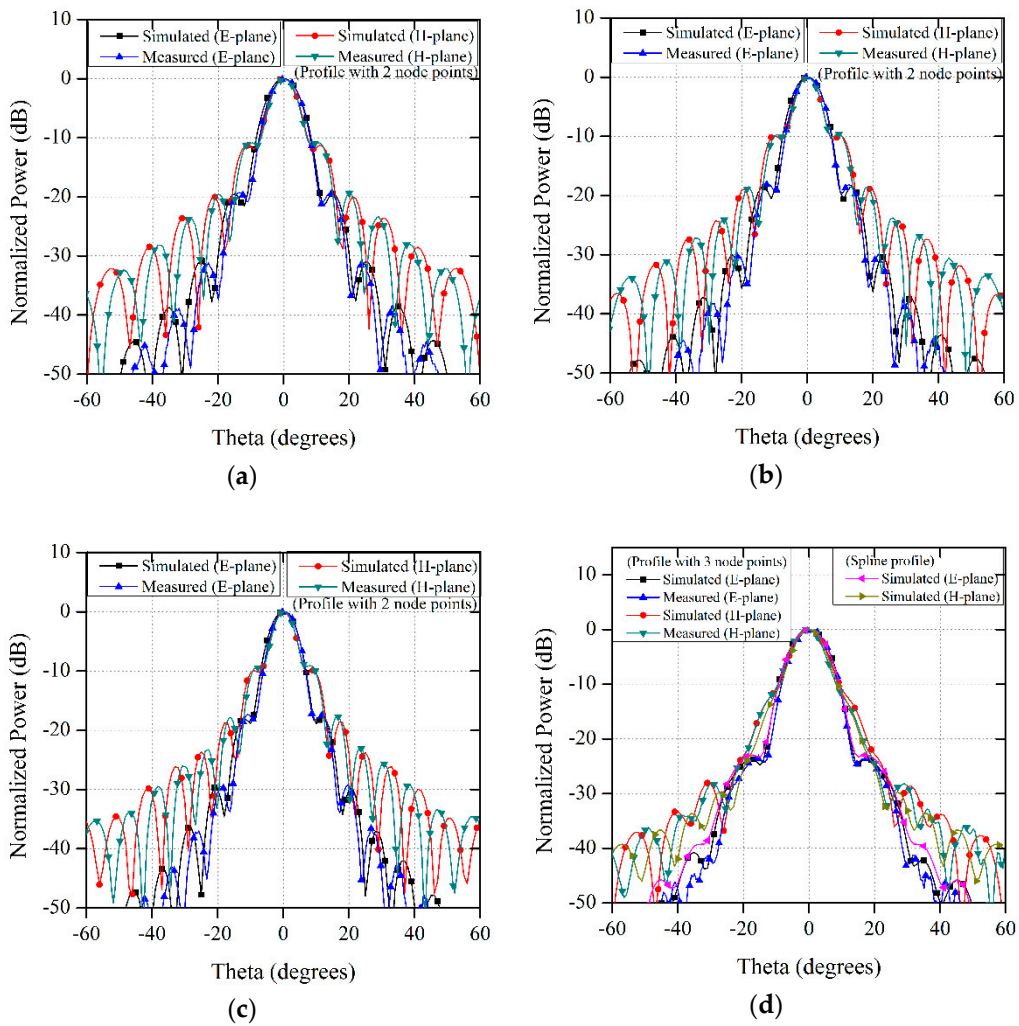


Figure 16. Cont.

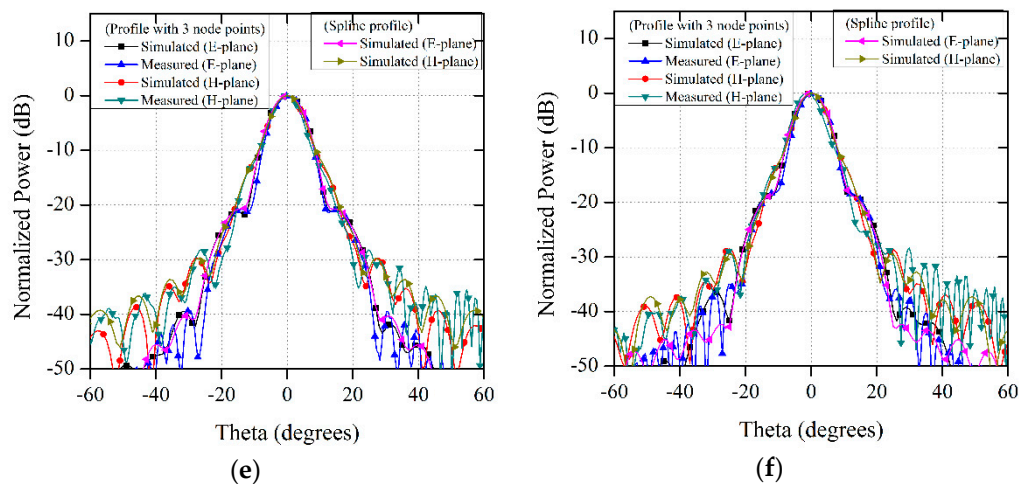


Figure 16. Comparison of simulated and measured radiation patterns for profiled horn antenna with 2 node points at (a) 50 GHz; (b) 55 GHz; (c) 60 GHz, profile with 3 node points and spline profile horn at (d) 50 GHz; (e) 55 GHz; (f) 60 GHz.

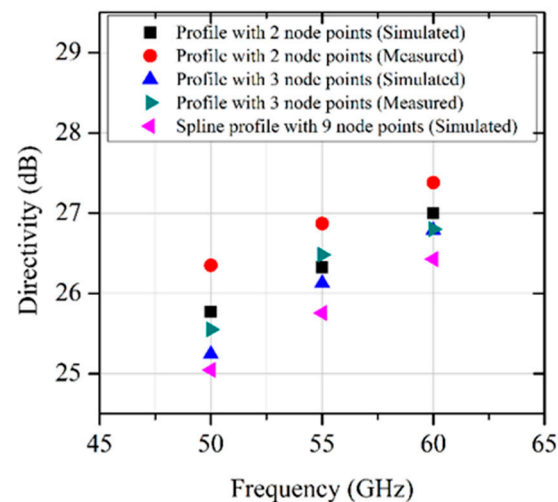


Figure 17. Comparison of simulated and measured directivity index (dB).

As seen from the results, the measured radiation patterns are very similar to the simulated ones for both profiles having 2 and 3 nodes. Moreover, the spline profile horn (having 9 node points) has a similar performance as that of the mirror image profile having 3 nodes since it has been designed with similar purposes. The measured directivity is in close agreement with that of the simulated results having the maximum uncertainty of ± 0.5 dB, as the measured one has been derived from the radiation pattern with only two phi cuts (at 0° and 90°). The measured directivity accuracy can definitely be improved (having uncertainty around ± 0.15 dB) in case of having the full spherical radiation pattern, measured with a higher number of phi cuts ($< 5^\circ$ step size). The 3 dB beamwidth can be estimated from the directivity and radiation patterns as for the metallic horn antenna. The measured radiation pattern for angles from 30 to 60 degrees has some noise but only for H-plane cut in the measured profile with three nodes. The reason for the noise may be the movement of absorbent material during rotation at the end of the measurement. In any case, we consider the results accurate enough to validate the proposed design in this paper.

6. Conclusions

A profiled smooth circular waveguide horn using piecewise biarc Hermite polynomial interpolation has been designed and fabricated. It has more degrees of freedom compared to the spline profile and less intermediate node points (one-third of the spline profile),

which reduces the optimization time and resources. As the polynomial interpolation profile is controlled by the vectors and not the radius of the intermediate node points, the limitation of the spline profile, i.e., successive node points having a smaller radius than that of the preceding ones, has been eliminated. Hence, the profile can be easily manufactured with electro erosion techniques, which are very suitable for millimeter-wave and even submillimeter-wave frequencies to reduce the manufacturing cost. Moreover, the performance of the proposed design can be optimized only by changing the location of the principal unit normal vector points. The S_{11} and radiation patterns have been measured and are in close agreement with the simulated results for both the scaled down V-band horn antennas (having 2 and 3 node points). A comparison has been made with a spline profile horn that needs at least 9 node points to achieve similar performance with an increase in computation complexity; this amount of node points adds. As a conclusive remark, Table 5 shows the comparison of the proposed horn antenna with the spline profiled horn [9].

Table 5. Resulting comparison of the proposed horn with spline profiled horn antenna.

Type of Horn Antenna	Number of Nodes	Frequency (GHz)	S_{11} (dB)	Radiation Pattern Optimization	Manufacturing with a Lathe	Manufacturing with EDM ¹
Spline profiled horn [9]	7	80–120 GHz	<−25	Time consuming due to many nodes	Difficult for frequencies higher than 50 GHz	Difficult or even not possible as the profile usually derives to have non-accessible zones
Spline horn ²	9	50–60 GHz	<−22	-	-	-
Proposed horn ³	3	50–60 GHz	<−22	Easy and fast	Difficult for frequencies higher than 50 GHz	Non-accessible zones are avoided

¹ Electrical discharge machining (EDM), also known as spark machining, spark eroding, die sinking, wire burning or wire erosion, is a metal fabrication process whereby a desired shape is obtained by using electrical discharges (sparks). ² To design the proposed profile using spline interpolation, it requires at least 9 nodes. ³ Having comparable performance to the spline profiled horn (with 9 nodes).

Author Contributions: Conceptualization, J.G.; methodology, J.G., D.P., and J.T.; software, J.G.; validation, J.G.; formal analysis, J.G., D.P., and J.T.; investigation, J.G.; resources, J.G., D.P., and J.T.; data curation, J.G., D.P., and J.T.; writing—original draft preparation, J.G.; writing—review and editing, J.G., D.P., and J.T.; visualization, J.G., D.P., and J.T.; supervision, D.P. and J.T.; project administration, J.G., D.P., and J.T.; funding acquisition, J.G., D.P., and J.T. All authors have read and agreed to the published version of the manuscript.

Funding: This research was funded by Visvesvaraya Ph.D. Scheme for Electronics and IT, Ministry of Electronics and Information Technology, Government of India, grant number MEITY-PHD-1363 and “The APC was funded by Public University of Navarra, Spain”. This research was funded by the Spanish State Research Agency, Project No. PID2019-109984RB-C43/AEI/10.13039/501100011033.

Acknowledgments: The authors of this paper are sincerely thankful to Nirma University, Ahmedabad, India, and to the Public University of Navarra, Pamplona, Spain, for the necessary support. Thanks are also due to the scientists of Space Applications Centre—Indian Space Research Organisation (SAC-ISRO), Ahmedabad, for providing the measurement facility.

Conflicts of Interest: The authors declare no conflict of interest. The funders had no role in the design of the study; in the collection, analyses, or interpretation of data; in the writing of the manuscript; or in the decision to publish the results.

References

- Olver, A.D.; Clarricoats, P.J.B.; Shafai, L.; Kishk, A.A. *Microwave Horns and Feeds*; No. 39; IET: London, UK, 1994.
- Potter, P.D. A new horn antenna with suppressed sidelobes and equal beam widths. *Microw. J.* **1961**, *6*, 71–78.
- Granet, C.; James, G.L. Design of corrugated horns: A primer. *IEEE Antennas Propag. Mag.* **2005**, *47*, 76–84. [[CrossRef](#)]
- Sharma, S.B.; Pujara, D.A.; Chakrabarty, S.B.; Singh, V.K. Improving the cross-polar performance of an offset parabolic reflector antenna using a rectangular matched feed. *IEEE Antennas Wirel. Propag. Lett.* **2009**, *8*, 513–516. [[CrossRef](#)]
- Lier, E.; Aas, J.A. Simple hybrid mode horn feed loaded with a dielectric cone. *Electron. Lett.* **1985**, *21*, 563–564. [[CrossRef](#)]

6. Lier, E. A dielectric hybrid mode antenna feed: A simple alternative to the corrugated horn. *IEEE Trans. Antennas Propag.* **1986**, *34*, 21–29. [[CrossRef](#)]
7. Chung, J.Y. Ultra-wideband dielectric-loaded horn antenna with dual-linear polarization capability. *Prog. Electromag. Res.* **2010**, *102*, 397–411. [[CrossRef](#)]
8. Lier, E. Hybrid-mode horn antenna with design-specific aperture distribution and gain. In Proceedings of the IEEE Antennas and Propagation Society International Symposium. Digest. Held in Conjunction with: USNC/CNC/URSI North American Radio Sci. Meeting (Cat. No. 03CH37450), Columbus, OH, USA, 22–27 June 2003; pp. 502–505. [[CrossRef](#)]
9. Granet, C.; James, G.L.; Bolton, R.; Moorey, G. A smooth-walled spline-profile horn as an alternative to the corrugated horn for wide band millimeter-wave applications. *IEEE Trans. Antennas Propag.* **2004**, *52*, 848–854. [[CrossRef](#)]
10. Lu, H.D.; Lv, X.; Gao, Z.J.; Liu, Y. Experimental radiation characteristics of micromachined terahertz low-profile corrugated horn antenna. *Microw. Opt. Technol. Lett.* **2015**, *57*, 364–367. [[CrossRef](#)]
11. Ying, Z.; Kishk, A.A.; Kildal, P.S. Broadband compact horn feed for prime-focus reflectors. *Electron. Lett.* **1995**, *31*, 1114–1115. [[CrossRef](#)]
12. Vishnu, G.J.; Jani, G.; Pujara, D. Design and optimization of a Ku-band compact axial corrugated horn antenna using ANFIS. In Proceedings of the 2016 International Symposium on Antennas and Propagation (APSYM), Cochin, India, 15–17 December 2016; pp. 1–4. [[CrossRef](#)]
13. Teniente, J.; Martínez, A.; Larumbe, B.; Ibáñez, A.; Gonzalo, R. Design guidelines of horn antennas that combine horizontal and vertical corrugations for satellite communications. *IEEE Trans. Antennas Propag.* **2015**, *63*, 1314–1323. [[CrossRef](#)]
14. Vishnu, G.J.; Jani, G.; Pujara, D.; Menon, S.S. U-band hybrid corrugated horn: An alternative to the conventional radial corrugated horns. In Proceedings of the 2017 IEEE Asia Pacific Microwave Conference (APMC), Kuala Lumpur, Malaysia, 13–16 November 2017; pp. 853–856. [[CrossRef](#)]
15. Granet, C.; James, G.L. Smooth-walled spline-profile Ka-band horn covering both the full commercial and military bands. *Microw. Opt. Technol. Lett.* **2008**, *50*, 2119–2121. [[CrossRef](#)]
16. Vishnu, G.J.; Pujara, D.A. Improving the performance of profiled conical horn using polynomial interpolation and targeting the region of interest. *Prog. Electromag. Res.* **2018**, *77*, 129–136. [[CrossRef](#)]
17. Vishnu, G.J.; Pujara, D.A.; Pandya, H. Design and Development of a D-Band Corrugated Horn Antenna for Millimeter-Wave Plasma Diagnostics. *Prog. Electromag. Res.* **2019**, *85*, 101–108. [[CrossRef](#)]
18. De Boor, C.; De Boor, C.; Mathématicien, E.U. *A Practical Guide to Splines*; Springer: New York, NY, USA, 1978; Volume 27, p. 325.
19. Birkhoff, G.; Schultz, M.H.; Varga, R.S. PiecewiseHermiteInterpolation in Oneand Two Variableswith Application to Partial Differential Equations. *Numerische Mathematik* **1968**, *11*, 232–256. [[CrossRef](#)]